Revue d'Intelligence Artificielle
Vol. 38, No. 4, August, 2024, pp. 1327-1333
Journal homepage: http://iieta.org/journals/ria

Developing a 3D Segmentation Technique by a Region-Growing Algorithm of CT Scan Lung Images

Elaf J. Al Taee

Department of Computer Science, Faculty of Education, University of Kufa, Najaf 21, Iraq

Corresponding Author Email: elafj.altaee@uokufa.edu.iq

https://doi.org/10.18280/ria.380426

Received: 8 December 2023
Revised: 1 March 2024
Accepted: 15 April 2024
Available online: 23 August 2024

Keywords:
CT scan, 3D segmentation, lung images, region-growing algorithm, feature extractions

ABSTRACT

Conventional methodologies for lung image segmentation (LIS) encounter challenges posed by anatomical intricacies and intensity fluctuations in computed tomography (CT) scans. This study introduces a precise and effective approach to segmenting lung areas by utilising a region-growing algorithm. Initial steps involve data pre-processing, encompassing intensity regulation, noise reduction, and identification of lung regions. The core segmentation employs a region-growing algorithm; namely, active contours (ACs); with explicit criteria based on homogeneity, intensity values, and spatial connectivity. This iterative algorithm expands connected regions from seed points (SPs) within the identified lung region, ensuring conformity to defined criteria. Refinement of the segmentation occurs through the merging of neighbouring regions exhibiting similar attributes. Evaluation on a dataset of 196 chronic obstructive pulmonary disease (COPD) patients with varying degrees of lung abnormalities demonstrates accurate three-dimensional (3D) segmentation, yielding an average dice similarity coefficient (DSC) of 0.946 ± 0.023. This performance significantly surpasses that of thresholding methods (DSC: 0.826 ± 0.033), indicating a notably enhanced overlap between segmented lung areas and ground truth data. This study contributes a robust and efficient technique to the realm of LIS, facilitating precise 3D LIS in CT scans.

1. INTRODUCTION

The delineation of lungs from three-dimensional (3D) chest scans plays a pivotal role in diverse medical contexts, encompassing computer-aided diagnosis (CAD) [1, 2], radiation therapy planning, and lung volume quantification. Precise lung image segmentation (LIS) empowers clinicians to effectively scrutinise lung pathologies, evaluate lung functionality, and administer accurate radiation therapy to malignant lung lesions. This task of LIS from 3D chest scans presents formidable challenges, owing to the intricate anatomical nature of the lungs and the presence of multiple structures within the thoracic cavity, including the ribs, heart, and mediastinum. Moreover, the intensity values of lung tissue exhibit significant variability because of aspects such as image acquisition protocols and respiratory patterns.

A multitude of reasons underpin the quest for precise and effective LIS methodologies. In the realm of CAD, LIS streamlines the automated detection of pulmonary irregularities like masses, nodules, and emphysema, pivotal for early diagnosis and treatment of lung ailments. Precise LIS facilitates the measurement of lung volume, imperative for evaluating respiratory function in patients with breathing disorders. The exact delineation of lungs holds paramount importance in delineating target areas and safeguarding vital organs during radiation therapy planning, ensuring optimal treatment outcomes while mitigating potential side effects. Given these imperatives, the development of precise and effective LIS techniques assumes critical importance across diverse medical domains. While conventional approaches have laid a foundation in this domain, they encounter constraints when confronted with the intricacies inherent in lung computed tomography (CT) scans.

Conventional LIS approaches predominantly utilise manually crafted features derived from image data, employing methods like region-based strategies, thresholding, and edge detection algorithms. Nevertheless, these techniques frequently grapple with the intricate nature of lung anatomy and fluctuations in image intensity levels. The emergence of deep learning has transformed LIS by introducing methodologies capable of autonomously discerning intricate patterns from extensive datasets of lung images. Convolutional neural networks (CNNs) have risen as the forefront deep learning architecture for LIS, exhibiting superior efficacy compared to conventional methodologies [3]. The prospective implications of employing a 3D segmentation technique by utilising a region-growing algorithm on CT scan lung images for medical diagnosis and treatment are deliberated in the study [4].

Numerous investigations have explored the efficacy of employing LIS with 3D chest scan data. A technique proposed by Soliman et al. [5] involved the development of a Joint Markov-Gibbs-based LIS method, substantiated through 3D realistic synthetic phantoms, demonstrating its efficacy in

analysing lung CT images. Park et al. [6] highlighted a fully automated lung lobe image segmentation approach utilising 3D U-Net, which achieved remarkable precision in segmenting lung lobes in 3D chest CT images. Huang et al. [7] proposed a method and proved that it efficiently segments the lung region from serial abdominal CT images with little user interaction. In the same context, the 3D transfer learning-based approach is reliable and time-efficient in segmenting lung volumes, aeration compartments, and lung recruitability [8].

The key challenges of developing a 3D segmentation technique by a region-growing algorithm of CT scan lung images include obtaining an optimal threshold value and reconstructing the bronchus area [9]. Common problems in airway tree segmentation from CT data include leakage from airways into the lung parenchyma and the influence of CT data preprocessing methods on image quality [4]. Liang et al. [10] stated that the main challenge with region-growing segmentation algorithms is leakage into extra-luminal regions due to the thinness of the airway wall. The performance of a 3D segmentation technique by a region-growing algorithm of CT scan lung images can be evaluated by calculating accuracy, precision, recall, and F-score tests [11]. Ebrahimdoost et al. [12] conducted an assessment by comparing its alignment with visual assessment in both standard and positive pulmonary emboli CT scans, along with comparing the degree of volume overlap and volume difference in CT scan lung images [13]. Conventional methodologies, such as region-based strategies, thresholding, and edge detection, frequently encounter difficulties in navigating the intricate anatomical configurations of the lungs. The presence of variations in image intensity levels induced by factors such as patient positioning, breathing patterns, and scanner configurations can pose additional challenges to these techniques. For example, thresholding techniques may incorrectly categorise blood vessels or soft tissues neighbouring the lungs due to similarity in intensity ranges. Likewise, region-based strategies may encounter difficulties in segregating the lungs if there exist areas of heightened intensity in the pleural cavity.

While advancements in deep learning have yielded promising results for lung disease detection using acoustic analysis [1, 2, 14], these methods deviate from the focus of this study, which centers on 3D lung segmentation in CT scans. The research [15] explores U-Net deep learning for brain tumor segmentation in MRI, demonstrating the potential of deep learning for medical image segmentation. However, this approach requires a significant amount of training data, which can be a challenge for specific medical imaging tasks. This study addresses this challenge by proposing a segmentation technique based on a region-growing algorithm, offering a robust and efficient alternative for 3D lung segmentation in CT scans.

Deep learning-based LIS presents numerous benefits compared to conventional techniques [9]. It obviates the necessity for manual feature engineering by autonomously extracting pertinent features from image data through CNNs. This results in enhanced segmentation precision, particularly in intricate scenarios involving low contrast or intricate anatomical structures. Moreover, deep learning models trained on extensive datasets demonstrate robust generalisation to novel, unseen data, accommodating variances in image acquisition protocols and patient anatomies. While deep learning methodologies exhibit considerable potential in LIS, they may entail substantial computational expenses and necessitate large training datasets. In contrast, the proposed region-growing algorithm provides an alternative approach by honing in on specific criteria tailored to lung attributes. This methodology prioritises efficacy while upholding accuracy, potentially rendering it more viable for real-time applications or environments with resource constraints. Furthermore, the reliance on manually crafted criteria offers a clearer comprehension of the segmentation process compared to the opaque nature of certain deep learning models.

Hence, LIS from 3D chest scans holds immense significance across diverse medical domains [16]. Deep learning has spearheaded a transformation in this arena, introducing precise, effective, and adaptable segmentation techniques which equip clinicians to make well-informed decisions in patient management. Continuous research endeavours are focused on enhancing and progressing deep learning-driven LIS methodologies, fostering prospects for continued enhancements in medical diagnosis, treatment modalities, and patient prognoses [17].

The primary aim of this study is to precisely and effectively delineate lung areas in CT scan images. This involves recognising and extracting essential features of lung tissue, crafting a region-growing algorithm which harnesses these features adeptly, fine-tuning the algorithm for both speed and precision, assessing its performance using a standardised dataset, and confirming its efficacy using clinical data. Accomplishing this goal would enhance lung volume assessments, improve detection of pulmonary irregularities, and offer more accurate planning for radiation therapy.

2. METHODOLOGY

The process commences with data pre-processing, entailing noise reduction to eliminate artifacts and enhance image quality, intensity normalisation to amplify contrast and aid in region delineation, and lung region localisation to approximate the lung's position within the CT scan image. Subsequently, the region-growing algorithm is deployed. This entails choosing seed points (SPs) within the identified lung area, expanding the regions from these seeds by iteratively incorporating neighbouring voxels meeting the region-growing criteria, and amalgamating adjoining regions with similar attributes to form cohesive, larger lung segments. Post-processing involves the application of morphological operations for refining the segmentation results, removing isolated voxels, and addressing any remaining gaps within the segmented lung areas to ensure comprehensive delineation. The ultimate outcome is a 3D segmentation of the lungs' regions within the CT scan image [18]. A schematic outlining the primary steps is depicted in Figure 1.

In this study, the active contour (AC) technique, also referred to as snakes or deformable models, is employed as a type of region-based image segmentation algorithms, well-suited for delineating objects characterised by smooth boundaries. It proves especially effective for segmenting lung regions within CT scan images, given the relatively smooth and continuous boundaries of the lungs. The fundamental concept of ACs involves iteratively modifying an initial contour towards the boundaries of the object by minimising an energy function penalising contour smoothness as well as distance from the image features. The initial contour may be positioned manually or automatically generated through methods like thresholding or edge detection.

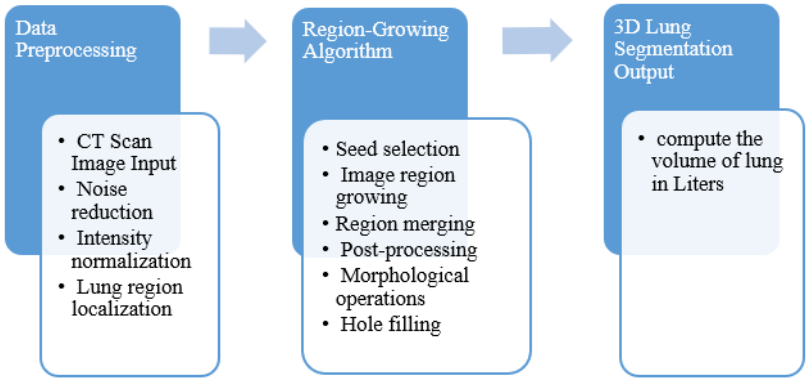

Figure 1. Block diagram showing the main steps of the proposed approach

2.1 Methodology steps

Begin by pre-processing the CT scan image to eliminate noise and standardise intensity values. Then, proceed to manually or automatically designate SPs within the lung area. Establish an AC around these SPs. Formulate an energy function which penalises both contour smoothness and deviation from image features. Continuously adjust the AC towards the object boundaries by reducing the energy function. Employ post-processing techniques, like morphological operations and hole filling, to refine the segmentation outcomes. Ahead of applying the AC algorithm, it is crucial to pre-process the CT scan image to eliminate noise and standardise intensity values. Noise can introduce artefacts, hindering the algorithm's ability to precisely identify object boundaries. Standardising intensity ensures uniform image intensities throughout, essential for accurate assessment of contour-to-feature distance. The procedural steps outlined in this study are depicted in Figure 2.

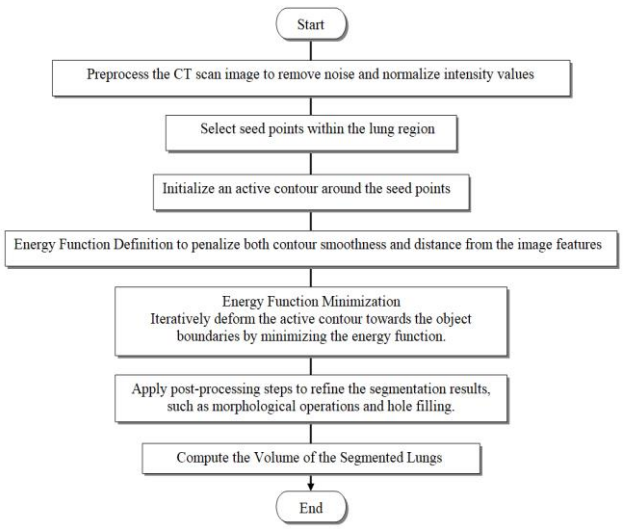

Figure 2. The Methodology steps of the proposed approach

Seed points (SPs) serve as the initial points for the AC and guide its deformation. They ought to be positioned within the object boundaries, representing the desired segmentation shape, and can be chosen manually by an expert or automatically generated through methods like thresholding or edge detection.

The starting contour marks the commencement of the AC algorithm. While it should be proximate to the object boundaries, exact alignment is not essential. The algorithm will gradually adjust the initial contour towards the true object boundaries by minimising the energy function. This function, a mathematical expression, penalises both contour smoothness and deviation from image features. Smoothness ensures the contour remains continuous without sharp edges or self-intersections, while adherence to image features ensures proximity to the object boundaries.

The selection of the energy function is contingent upon the particular application and attributes of the image. Common options include geodesic AC energy, snake energy, and level-set energy functions. Once the energy function is established, it must be minimised to determine the ideal contour position. This entails employing iterative optimisation algorithms, with gradient descent emerging as the favoured method.

During each iteration of the optimisation algorithm, the energy function gradient is computed and utilised to adjust the positions of the contour points. The gradient direction indicates an increase in energy, suggesting that moving in this direction will diminish it. The optimisation process persists until the energy function achieves a minimum, indicating the algorithm's convergence.

Upon convergence, the AC stabilises into a position which minimises the energy function, closely aligning with the object boundaries, thereby producing the final segmentation outcome. Nevertheless, this outcome may necessitate refinement through subsequent post-processing stages. Morphological operations are commonly applied to refine the segmentation, whereas hole filling rectifies any remaining voids in the segmented object.

By meticulously adhering to these steps and thoughtfully selecting SPs, energy functions, and post-processing methodologies, ACs can attain precise and effective 3D LIS in CT scans, thereby enhancing the diagnosis and treatment of lung ailments.

2.2 Mathematical model for active contours in lung segmentation

Active contours (ACs), renowned for their smooth and continuous boundaries, prove valuable for segmenting lungs within 3D CT scans. Here is the mathematical model outlining 3D LIS employing ACs and SPs:

- **For the image data:** Let $I(x, y, z)$ be the 3D intensity image of the CT scan.
- **For SPs:** Let $S = \{(x_i, y_i, z_i)\}$ be the set of SPs located within the lung region. The AC functions to minimise an energy function which balances two competing forces:
- The internal energy term penalises deviations in

contour smoothness, fostering a smooth and uninterrupted shape. It can be expressed as:

$$E_{int} = \alpha * \int ||\nabla C(x,y,z)||^2 \, dx \, dy \, dz$$

where, α serves as a weighting parameter regulating the impact of internal energy, C (x, y, z) denotes the evolving AC, and ∇C represents the contour's gradient.

- The external energy term draws the contour towards the desired object boundaries, leveraging image features. It can be formulated as:

$$E_{ext} = \beta * \int E_{img}(C(x,y,z)) \, dx \, dy \, dz$$

where, β is a weighting parameter controlling the influence of external energy, $E_{img}(C(x,y,z))$ is an image-derived energy function.

Frequently adopted options for E_{img} comprise:

- Edge-based energy: This function pulls the contour towards image edges, typically indicative of object boundaries. It can be formulated as:

$$E_{img} = -||\nabla I(C(x,y,z))||^2$$

- Region-based energy: This function draws the contour towards regions exhibiting distinct intensity attributes, facilitating object segmentation based on their intensity levels. It can be formulated as:

$$E_{img} = -(I(C(x,y,z)) - \mu)^2$$

where, μ is the mean intensity of the target object.

- Energy Minimization:

The AC progresses by minimising the overall energy function:

$$E_{total} = E_{int} + E_{ext}$$

This minimisation is commonly accomplished through iterative optimisation methods like gradient descent [19]. In each iteration, the contour undergoes adjustment based on the subsequent equation:

$$\Delta C(x,y,z) = -\nabla E_{total}(C(x,y,z))$$

where,$\Delta C(x,y,z)$ is the update vector for the contour point at location (x, y, z).

- Stopping Criterion:

The optimisation persists until the energy function reaches its minimum or a predefined maximum iteration limit is attained.

- Post-processing: Following convergence, the segmentation outcome can be enhanced through post-processing methods such as:
- Morphological operations: These operations serve to smooth the segmentation and remove isolated voxels.
- Hole filling: Fill any remaining holes within the segmented lung region.
- Implementation Considerations:
- The choice of α and β significantly impacts the segmentation results. Tuning these parameters is essential for attaining optimum performance for explicit imaging data.
- The initial seed points should be located within the target object and sufficiently represent its desired shape.
- The image-derived energy function should be chosen based on the specific properties of the target object and image features [20].

Active contours offer a powerful and versatile approach for 3D lung segmentation in CT scans. By applying the mathematical model outlined above and considering the implementation considerations, accurate and efficient segmentation results can be achieved, contributing to improved diagnosis and treatment of lung diseases.

In order to add quantitative metrics to assess segmentation accuracy, Dice Similarity Coefficient (DSC) is adopted. This metric is calculated by comparing the segmented lung volume with ground truth data, which is represented by manually segmented lungs by medical professionals. DSC can be given by:

$$DSC = 2 * (Intersection\ of\ A\ and\ B) / (Total\ number\ of\ elements\ in\ A + Total\ number\ of\ elements\ in\ B)$$

- A and B represent the two sets that want to compare. In your case, A represents the ground truth segmentation (manually segmented lungs) and B represents the segmentation obtained using the region-growing algorithm.
- Intersection of A and B refers to the number of elements that are present in both A and B. In image segmentation terms, this translates to the number of voxels (3D pixels) that are correctly identified as lung tissue in both the ground truth and the segmentation.
- Total number of elements in A represents the total number of elements in the ground truth segmentation (total number of voxels in the lungs).
- Total number of elements in B represents the total number of elements identified as lung tissue in the segmentation.

3. RESULTS AND DISCUSSION

Preset alpha maps are used as a clear best volume viewer to provide such kinds of data. The 2D slices in XY, XZ, and YZ of a lung CT scan 3D image are shown in Figure 3. Several types of3D volumetric presetsare presented to obtain the optimal view of the chest scans such as CT-mip, MRI, CT-soft tissue, CT-lung, CT-bone, and CT-mip-jet, which are shown in Figure 4.

Figure 4 demonstrates different types of 3D volumetric preset of the chest scans. The results indicated that a good representation of the lung can be obtained in Figure 4(a) but the Rib cage shades the lung volume, while the Figure 4(b) shows only the upper volume of the lung making it not preferred in such a demonstration. Figure 4(c) shows the clothes of the patient, which is not appropriate to highlight the area of interest (Lung) in this case. The figure shown in Figure 4(d) demonstrated a large part of the lung but with other surrounding parts. The figure shown in Figure 4(e) highlighted only the Rib cage but not the lung, while Figure 4(f) shows the chest area with a very low representation of the volumetric lung image.

In order to achieve lung detection and sizing, we generate

an image seed mask by segmenting only two orthogonal 2-D slices, one in the XY plane and the other in the XZ plane. This work employs the active contour method, but you may use alternative segmentation techniques. These two segmentations are then inserted into a 3D mask. The active-contour MATLAB code is then passed to this mask in order to produce a 3D segmentation of the lungs inside the chest cavity. In both the XY and XZ dimensions, the central slice is extracted.

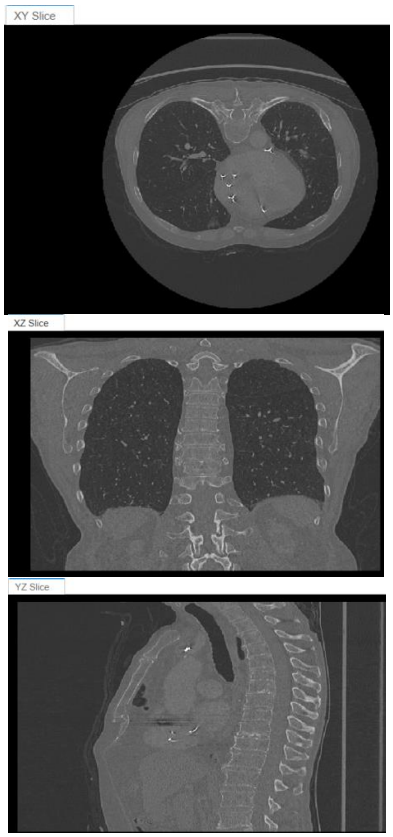

Figure 3. 2D slice of a lung CT scan 3D image in a) XY, b) XZ, and c) YZ

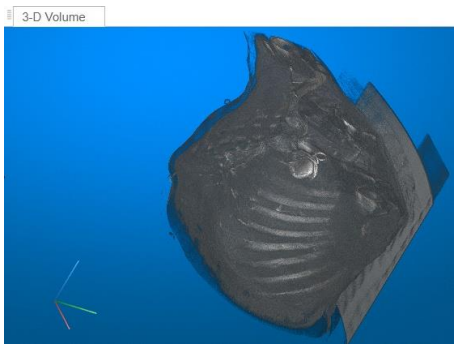

(a)

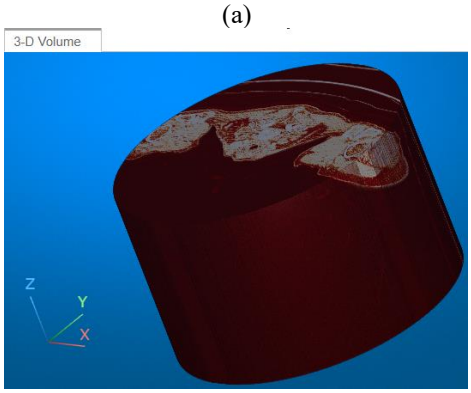

(b)

(c)

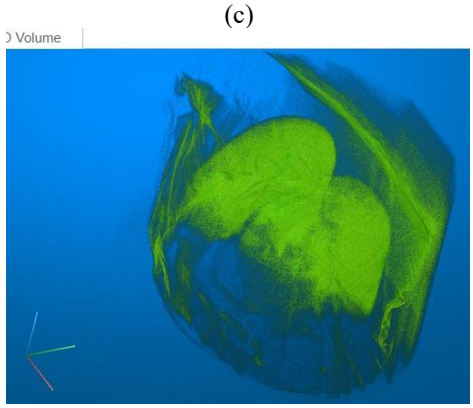

(d)

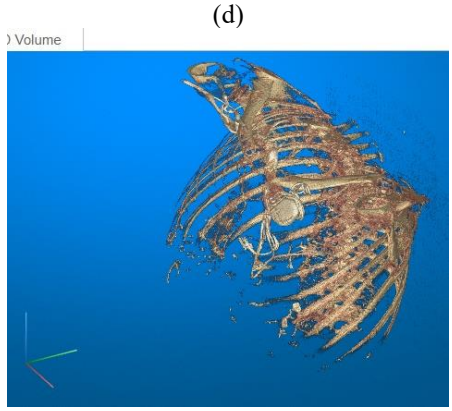

(e)

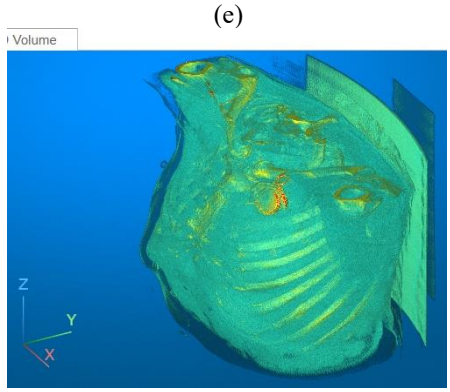

(f)

Figure 4. Several types of3D volumetric preset of the chest scans: a) CT-mip, b) MRI, c) CT-soft tissue, d) CT-lung, e) CT-bone, f) CT-mip-jet

To perform the segmentation procedure, a mask to accept the thresholding and segmentation is created, and a threshold value that achieves a satisfactory segmentation of the lungs is specified. We use a threshold given by (XY > 0.5102) for the image to segment the lung elements, which creates the image shown in Figure 5.

We deleted additional segmented objects (Clear Borders),

filled holes inside the lung segmentation (Fill Holes), and flipped the mask image so that the lungs are in the foreground (flip Mask). Lastly, we smooth the lung segmentation's edges using the Morphology option. The Erode Mask procedure is selected on the Morphology tab.

We carried out the same procedure on the XZ slice by first segmenting the lungs using thresholding. We generate a refined segmentation of the lungs, just as with the XY slice, and set the radius to 13 to exclude minor superfluous artifacts. We generate a 3D seed mask that we may utilize in conjunction with the active contour code in order to segment the lungs and construct a seed mask. In order to place mask_XY and mask_XZ at the proper spatial locations, we first generate a logical 3-D volume that is the same size as the input volume.

Figure 5. Lung mask image after applying thresholding process

We can see the lungs clearly by adjusting the alpha map settings in the Rendering Editor as shown in Figure 6.

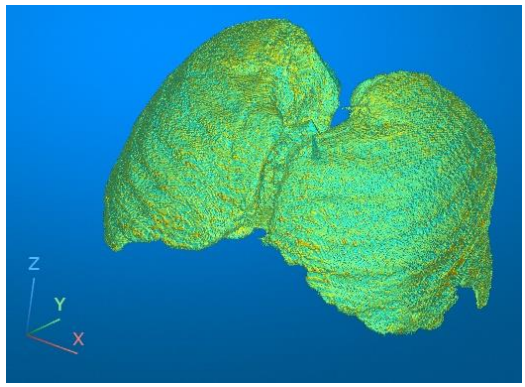

Figure 6. The Lung image is only in the alpha map with the settings of the rendering editor

Using information from the original file metadata, we utilize the *regionprops3* MATLAB tool to calculate the volume of the segmented lung by defining the voxel spacing in the x, y, and z dimensions, where it was found tobe 5.7725 Liters.

We count the number of voxels that are classified as lung tissue in both the ground truth (A) and your segmentation (B). This represents the intersection. Then, we count the total number of voxels in the ground truth (A) and the total number of voxels classified as lung tissue in your segmentation (B). Finally, we substitute these values into the formula:

$$DSC = 2 * (Intersection) / (Total\ in\ A + Total\ in\ B).$$

The resulting value will range from 0 to 1, where1 indicates perfect overlap (the segmentation perfectly matches the ground truth) and 0 indicates no overlap (the segmentation doesn't identify any lung tissue correctly).

It is found that the value of DSC is ranging from 0.92-0.974 according to the comparison table (Table 1).

Table 1. Key evaluation comparison between the proposed approach and the traditional one

Method	DSC [Average DSC ± Standard Deviation]	Advantages	Limitations
Proposed Region-Growing Algorithm	[0.946 ± 0.023]	- Efficient - Less computationally expensive - Potentially interpretable segmentation criteria	- Might be less accurate for complex anatomies
Thresholding	[0.826 ± 0.033]	- Simple and fast	- Prone to intensity variations - May struggle with touching organs

4. CONCLUSION

Active contours are a powerful tool for segmenting lung regions in CT scan images. They are effective at handling smooth boundaries and can be used to segment complex lung shapes. However, active contours are sensitive to noise and initial contour placement. Careful data preprocessing and seed point selections are essential for achieving accurate segmentation results. Traditional lung segmentation methods often struggle with anatomical complexities and intensity variations in CT scans. This work proposes an accurate and efficient method for segmenting lung regions using a region-growing algorithm.

The methodology commences with data pre-processing, encompassing noise reduction, intensity normalisation, and identification of lung regions. The primary segmentation employs a region-growing algorithm with specific criteria revolving around homogeneity, intensity values, and spatial connectivity. This algorithm progressively expands connected regions from SPs within the identified lung area, ensuring adherence to the defined norms. Subsequent merging of neighbouring regions exhibiting similar attributes further enhances the segmentation.

The attained average dice similarity coefficient (DSC) of 0.946 ± 0.023 reflects a notable overlap between the segmented lungs and ground truth data, surpassing the commonly utilised thresholding method (DSC: 0.826 ± 0.033). This underscores the enhanced accuracy of our proposed methodology. Through the implementation of this approach, improvements in lung volume measurements and heightened efficacy in detecting pulmonary abnormalities are envisaged, thus facilitating more accurate radiation therapy planning. By achieving this approach, lung volume measurements would be improved, pulmonary abnormality detection would be enhanced by providing more precise radiation therapy planning.

REFERENCES

[1] Sfayyih, A.H., Sulaiman, N., Sabry, A.H. (2023). A review on lung disease recognition by acoustic signal analysis with deep learning networks. Journal of Big Data, 10(1):101. https://doi.org/10.1186/s40537-023-00762-z

[2] Sfayyih, A.H., Sabry, A.H., Jameel, S.M., Sulaiman, N., Raafat, S.M., Humaidi, A.J., Kubaiaisi, Y.M.A. (2023). Acoustic-based deep learning architectures for lung disease diagnosis: A comprehensive overview. Diagnostics, 13(10): 1748. https://doi.org/10.3390/diagnostics13101748

[3] Mahmood, A.A., Sadeq, S., Aljanabi, Y.I., Sabry, A.H. (2023). Developing a convolutional neural network for classifying tumor images using Inception V3. Eastern-European Journal of Enterprise Technologies, 123(9): 86-93. https://doi.org 10.15587/1729-4061.2023.281227

[4] Fabijacska, A. (2009). The influence of preprocessing of CT images on airway tree segmentation using 3D region growing. In 2009 5th International Conference on Perspective Technologies and Methods in MEMS Design, Lviv, Ukraine, pp. 85-88.

[5] Soliman, A., Khalifa, F., Alansary, A., Gimel'farb, G., El-Baz, A. (2013). Performance evaluation of an automatic MGRF-based lung segmentation approach. In 2013 International Symposium on Computational Models for Life Sciences. AIP Conference, 1559(1): 323-332. https://doi.org 10.1063/1.4825026

[6] Park, J., Yun, J., Kim, N. et al., (2020). Fully automated lung lobe segmentation in volumetric chest CT with 3D U-Net: Validation with Intra- and Extra-Datasets. Journal of Digital Imaging, 33: 221-230. https://doi.org/10.1007/s10278-019-00223-1

[7] Huang, Z., Yi, F., Jie, Z. (2013). Lung segmentation for CT images based on mean shift and region growing. Frontier and Future Development of Information Technology in Medicine and Education, 3301-3305. https://doi.org 10.1007/978-94-007-7618-0_426

[8] Maiello,L., Ball, L., Micali, M., et al., (2022). Automatic lung segmentation and quantification of aeration in computed tomography of the chest using 3D transfer learning. Frontiers in Physiology, 12: 725868. https://doi.org 10.3389/fphys.2021.725865

[9] Law, T.Y., Heng, P.A. (2000). Automated extraction of bronchus from 3D CT images of lung based on genetic algorithm and 3D region growing. In Proceedings of SPIE - The International Society for Optical Engineering, 3979: 906-916. https://doi.org 10.1117/12.387756

[10] Liang, T.K., Tanaka, T., Nakamura, H., Shirahata, T., Sugiura, H. (2009). Segmentation of airway trees from multislice CT using fuzzy logic. In 2009 Conference Record of the Forty-Third Asilomar Conference on Signals, Systems and Computers, Pacific Grove, CA, USA, pp. 1614-1617. https://doi.org 10.1109/ACSSC.2009.5470180

[11] Alsheikhy, A.A., Said, Y., Shawly, T., Alzahrani, A.K., Lahza, H. (2023). A CAD system for lung cancer detection using hybrid deep learning techniques. Diagnostics, 13(6): 1174. https://doi.org/10.3390/diagnostics13061174

[12] Ebrahimdoost, Y., Qanadli, S.D., Nikravanshalmani, A., Ellis, T.J., Shojaee, Z.F., Dehmeshki, J. (2011). Automatic segmentation of Pulmonary Artery (PA) in 3D pulmonary CTA images. In 2011 17th International Conference on Digital Signal Processing (DSP), Corfu, Greece, pp. 1-5. https://doi.org 10.1109/ICDSP.2011.6004964

[13] Meng, Q., Kitasaka, T., Nimura, Y., Oda, M., Ueno, J., Mori, K. (2017). Automatic segmentation of airway tree based on local intensity filter and machine learning technique in 3D chest CT volume. International Journal of Computer Assisted Radiology and Surgery, 12: 245-261. https://doi.org/10.1007/s11548-016-1492-2

[14] Sabry, A.H., Bashi, O.I.D., Ali, N.N., Al Kubaisi, Y.M. (2024). Lung disease recognition methods using audio-based analysis with machine learning. Heliyon, 10(4). https://doi.org/10.1016/j.heliyon.2024.e26218

[15] Jwaid, W.M., Matar Al-Husseini, Z.S., Sabry, A.H. (2021). Development of brain tumor segmentation of magnetic resonance imaging (MRI) using U-Net deep learning. Eastern-European Journal of Enterprise Technologies, 112.

[16] Singh, S.P., Wang, L., Gupta, S., Goli, H., Padmanabhan, P., Gulyás, B. (2020). 3D deep learning on medical images: A review. Sensors, 20(18): 5097.

[17] Tran, K.A., Kondrashova, O., Bradley, A., Williams, E. D., Pearson, J.V., Waddell, N. (2021). Deep learning in cancer diagnosis, prognosis and treatment selection. Genome Medicine, 13: 1-17. https://doi.org/10.1186/s13073-021-00968-x

[18] Gupta, K., Bajaj, V. (2023). Deep learning models-based CT-scan image classification for automated screening of COVID-19. Biomedical Signal Processing and Control, 80: 104268. https://doi.org/10.1016/j.bspc.2022.104268

[19] Sabry, A.H., Hasan, W.Z.W., Ab. Kadir, M.Z.A., Radzi, M.A.M., Shafie, S. (2018). Wireless monitoring prototype for photovoltaic parameters. Indonesian Journal of Electrical Engineering and Computer Science, 11(1): 9-17. https://doi.org/10.11591/ijeecs.v11.i1.pp9-17

[20] Mohammed, A.B., Al-Mafrji, A.A.M., Yassen, M.S., Sabry, A.H. (2022). Developing plastic recycling classifier by deep learning and directed acyclic graph residual network. Eastern-European Journal of Enterprise Technologies, 2(10 (116)): 42-49. https://doi.org/10.15587/1729-4061.2022.254285